Research Article Vol. 4, No. 3 / 15 March 2021 / OSA Continuum 911

Femtosecond infrared supercontinuum generation in 6H-SiC crystal

AGNĖ ŠUMINIENĖ,* VYTAUTAS JUKNA, ROSVALDAS ŠUMINAS, GINTARAS TAMOŠAUSKAS, AND AUDRIUS DUBIETIS

Laser Research Center, Vilnius University, Saulėtekio Ave. 10, LT- 10223, Vilnius, Lithuania
agne.suminiene@ff.stud.vu.lt

Abstract: We report on supercontinuum generation in silicon carbide (6H-SiC), pumped by tunable femtosecond pulses in the wavelength range of 1.3 - 2.4 μm, which cover the regions of normal, zero, and anomalous group velocity dispersion of the material. More than an octave spanning infrared supercontinuum spectra were measured, demonstrating almost constant blue cut-offs around 0.9 μm. Low energy thresholds for supercontinuum generation (depending on the pump wavelengths, but generally below 200 nJ) were demonstrated due to large nonlinear refractive index of the material ($n_2 = 97 \pm 19 \times 10^{-16}$ cm^2/W), which was experimentally evaluated by measurement of the nonlinear transmission at 2.0 μm.

1. Introduction

Ultrashort, ultrabroadband laser pulses in the near- and mid-infrared spectral region are on demand for applications in vibrational spectroscopy and for development of optical parametric chirped pulse amplification and pulse compression techniques [1–5]. Femtosecond supercontinuum (SC) generation in solid-state media is a unique nonlinear phenomenon which currently serves as a robust and well-established technique for producing ultrabroadband coherent radiation in the optical range [6,7]. Typically, supercontinuum generation is performed in wide-bandgap dielectric crystals, out of these, sapphire and YAG serve as most common and most reliable nonlinear materials [8,9]. For what concerns supercontinuum generation in sole infrared spectral range, narrow-bandgap dielectric crystals such as mixed thallous halides (KRS-5 and KRS-6) [10–12], and strontium barium niobate (SBN) [13] were shown to provide a viable alternative. More than that, semiconductor crystals have emerged as promising nonlinear materials for that purpose due to a combination of attractive optical properties such as large nonlinear index of refraction, wider transparency into the mid-infrared and zero group velocity dispersion (GVD) wavelengths that are shifted to the longer wavelengths compared to dielectrics. So far, supercontinuum generation via femtosecond filamentation has been demonstrated in bulk semiconductor crystals such as ZnS, ZnSe [14–18] and Si [19] where multioctave SC spectra extending from the near- to mid-infrared range were produced.

Silicon carbide (SiC) is a semiconductor material with high potential for hosting nonlinear interactions in this spectral region. In nonlinear photonics, SiC, as compared to silicon, has a considerable advantage due to its more than twice larger bandgap and hence the reduced nonlinear absorption in the near and mid-infrared spectral range. SiC can be grown in over 200 polytypes with different optical parameters and crystalline structures. However, the three commonly used and widely available polytypes are 3C-, 4H-, and 6H-SiC, with the former one being cubic, and the latter two hexagonal, uniaxial crystals. More importantly, 4H-SiC and 6H-SiC possess relatively large second-order nonlinearities [20]. More recently, dispersion of third-order nonlinearities has been calculated for the three SiC polytypes unveiling a large nonlinear refractive index, comparable to that of silicon: the obtained values were within the range from 0.5 to 6.3 $\times 10^{-14}$ cm^2/W in the 0.5-5 μm spectral region [21]. Experiments exploiting

#419234 https://doi.org/10.1364/OSAC.419234
Journal © 2021 Received 7 Jan 2021; revised 5 Feb 2021; accepted 8 Feb 2021; published 25 Feb 2021

OSA CONTINUUM

large second and third order nonlinearities of SiC demonstrated spectral broadening [22] and optical parametric oscillation [23] in waveguide and microresonator geometries, respectively, and broadband difference frequency generation [24] and optical parametric amplification [25] in bulk.

In this paper we study supercontinuum generation in 6H-SiC with femtosecond wavelength tunable laser pulses. We demonstrate that smooth supercontinuum spectra with fairly stable cut-off wavelengths around 0.9 μm are generated when tuning the wavelength of pump pulses from normal to anomalous GVD region of the crystal. We also measure the nonlinear transmission of the light filament in 6H-SiC sample which is then used to estimate the nonlinear refractive index of the material at 2 μm.

2. Experimental methods and parameters

The experiments were performed using an optical parametric amplifier (OPA, Topas-Prime, Light Conversion) pumped by an amplified Ti:sapphire laser system (Spitfire-PRO, Newport-Spectra Physics). In the experiment either signal or idler wave from the OPA was used, providing the tuning range of the pump pulses from 1.2 to 2.4 μm. The experimental setup is sketched in Fig. 1. The pump pulses were loosely focused by a BaF_2 lens (L) with a focal length f = 100 mm onto the front face of the 5 mm-thick 6H-SiC sample with the optical axis aligned perpendicular to the propagation direction of the incident beam. Variable neutral density filter (VDF) allowed fine tuning of the pump pulse energy at the entrance of the sample. The output face of the sample was imaged onto the input slit of a home built scanning prism spectrometer (SPS) using a pair of silver-coated parabolic mirrors positioned in a 4f imaging setup. The SPS was equipped with Si and InAsSb detectors enabling an effective detection range of 0.2 - 5.8 μm. For energy transmission measurements, a fraction of the pump beam energy was reflected from a thin fused silica plate (P) and directed to a PbSe detector (RD), which served as a reference, whereas the output beam was directed into a pyroelectric detector (D).

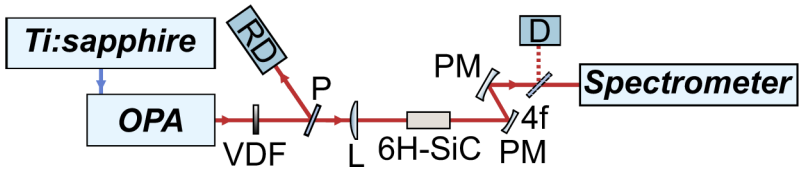

Fig. 1. Schematic of the experiment: VDF - variable neutral density filter, P - fused silica plate, RD - reference PbSe detector, L - lens, PM - parabolic mirror, D - pyroelectric detector.

Table 1 presents the relevant parameters of 6H-SiC crystal which are compared with other nonlinear media used for supercontinuum generation in the near to mid-IR spectral range. 6H-SiC possesses a useful combination of linear and nonlinear optical properties: a reasonable transparency range, large nonlinear refractive index and high optical damage threshold, that could be readily exploited for observation of filamentation phenomena and SC generation in particular. First of all, considering the bandgap of 6H-SiC, three to five photon absorption is expected in the range of available pump wavelengths, thus satisfying the threshold condition ($K \geq 3$ where K is the order of multiphoton absorption) for SC generation [26]. Secondly, compared to YAG, the bandgap of 6H-SiC is a few times smaller, which as a general rule of thumb, indicates that its optical damage threshold is significantly (around five times) lower. However, this is outweighed by the fact that the nonlinear index of refraction is expected to be around 15 times larger than that of YAG, which suggests a much lower critical power for self-focusing and hence the energy threshold for SC generation. Thirdly, the zero GVD wavelength of 6H-SiC is at 2.1 μm allowing the access to femtosecond filamentation in the anomalous GVD regime, characterized by simultaneous compression in space and time and light-bullet formation [27], which in turn yields generation of ultrabroadband, multioctave SC [28,29].

OSA CONTINUUM

Table 1. Main parameters of 6H-SiC and some other nonlinear media used for supercontinuum generation in the near to mid-infrared: E_g is the energy bandgap, T is the transmission range, n_0 and n_2 are linear and nonlinear refractive indexes, respectively, λ_0 is the zero GVD wavelength, DT is the optical damage threshold for femtosecond pulses. The bandgap and transmission parameters together with damage thresholds for Si and ZnSe were taken from [30]. Linear refractive index values are given for 2 μm. 6H-SiC and ZnSe nonlinear refractive index values were estimated using the van Stryland analysis at 2 μm [31]. The references to other parameter values are given in the table.

Material	E_g (eV)	T (μm)	n_0	λ_0 (μm)	$n_2 \times 10^{-16}$ (cm^2/W)	DT (J/cm^2)
6H-SiC	2.6	0.5-4	2.5537(o); 2.5873(e) [24]	2.1	86	0.60 [32]
Si	1.12	1.1-6.5	3.4401 [33]	>23	270 [34]	0.55
ZnSe	2.71	0.5-20	2.4318 [35]	4.8	74	0.53
YAG	6.5	0.21-5.2	1.8005 [36]	1.6	6.2 [37]	3 [38]

3. Results and discussion

Figure 2 shows the dynamics of spectral broadening versus the pump pulse energy measured using 93 fs pulses with a central wavelength of 2 μm, which falls close to the zero GVD wavelength of 6H-SiC. An explosive spectral broadening is observed above the threshold energy of 73 nJ, where a smooth SC spectrum spanning almost the entire near-IR spectral region and extending into the mid-infrared is produced. The low SC generation energy threshold is determined by the large nonlinear refractive index of 6H-SiC, see Table 1. A fairly constant width of the SC spectrum is maintained with further increase of the pump pulse energy, until a second burst of spectral broadening is observed at approximately 180 nJ, accompanied by spectral modulation that indicates the refocusing of the filament.

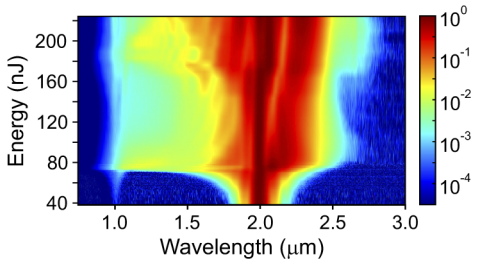

Fig. 2. Measured dynamics of spectral broadening in 6H-SiC crystal recorded with 93 fs, 2 μm pump pulses as a function of pulse energy. Logarithmic intensity scale is used in order to highlight fine spectral features.

Below the SC generation threshold, a faint but clearly distinguishable signal with a center wavelength around 1 μm is observed, which is attributed to phase-mismatched second harmonic generation. Since 6H-SiC is a positive uniaxial crystal, the pump pulse polarization was intentionally set to be ordinary to minimize second harmonic generation in order to avoid spectral "contamination". It should be noted that at the OPA output the signal (1.3 and 1.5 μm) and the idler (2.0 and 2.4 μm) waves are of orthogonal polarizations due to type-II phase matching in the OPA crystal. Therefore, the polarization of the idler wave was rotated by 90 degrees (by means of a periscope) to be identical to that of the signal wave (to be ordinarily polarized in 6H-SiC sample) in order to have the same SC pump polarization that suppresses second harmonic generation with all used pump wavelengths.

Figure 3 presents the SC spectra measured with four different wavelengths: 1.3, 1.5, 2.0 and 2.4 μm, and using pump pulse energies of 55, 70, 90 and 180 nJ, respectively, at which the spectral broadening saturates without filament refocusing. Notice an apparent change of the width and the

OSA CONTINUUM

shape of SC spectra from the red-shifted to symmetric and eventually to the blue-shifted, when the pump wavelength is tuned from normal to anomalous GVD regions of the nonlinear material [the zero GVD wavelength is 2.1 μm, see Fig. 4(a)]. More specifically, with 1.3 μm pump pulses, the measured SC spectrum exhibits a red-shift and covers the wavelength range from 0.85 to 2.13 μm, as evaluated at the 10^{-4} intensity level, see Fig. 3(a). A slightly broader and symmetric SC spectrum in the wavelength range of 0.87-2.40 μm was produced with 1.5 μm pump pulses, as shown in Fig. 3(b). The broadest SC spectra with strongly pronounced blue-shifts were measured in the regions of near-zero and anomalous GVD, with pump wavelenghts of 2.0 and 2.4 μm, as illustrated in Figs. 3(c) and 3(d), respectively. In the first case, the SC spectrum covers the 0.91-2.75 μm wavelength range, while in the latter case the SC spectrum extends from 0.92 to 3.21 μm and spans 1.8 optical octaves. The shapes of all measured SC spectra are smooth and do not contain any significant dips or detached peaks. Also note the generally low energies of the pump pulses (varying from 55 to 180 nJ) required to achieve a fully evolved spectral broadening without the onset of filament refocusing. The apparent increase of the pump pulse energy with the wavelength follows fairly well the square wavelength dependence of the critical power for self-focusing.

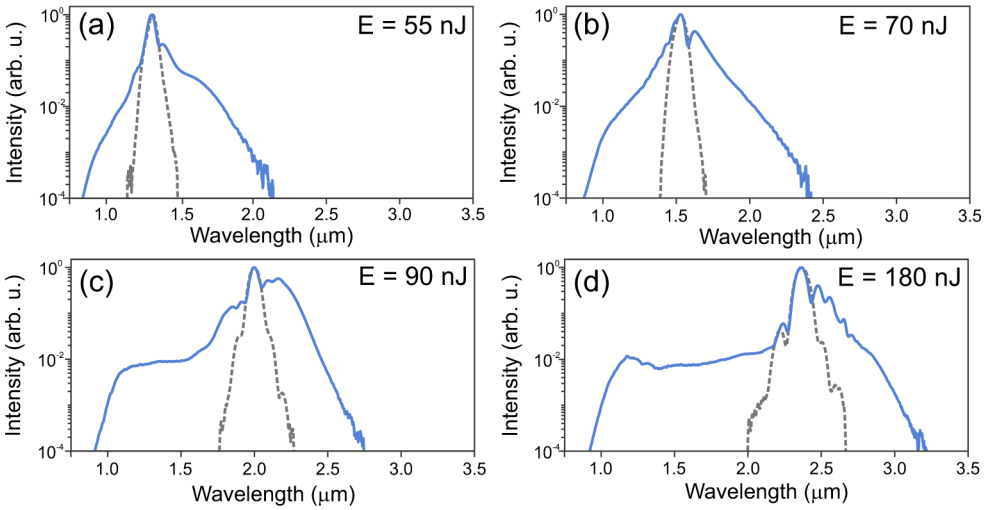

Fig. 3. Supercontinuum spectra generated in 6H-SiC using pump pulses with wavelengths of (a) 1.3 μm, (b) 1.5 μm, (c) 2.0 μm, and (d) 2.4 μm. The energies of the pump pulses are indicated within the figures. The input spectra are depicted by grey dashed curves.

The results are summarized in Fig. 4. Figure 4(a) illustrates the GVD curve of 6H-SiC, indicating the wavelengths at which the whole set of spectral measurements was performed. Figure 4(b) shows the measured SC blue-shifts defined at the 10^{-4} intensity level as a function of the pump pulse wavelength. The increase of the spectral blue shift with the increase of the pump wavelength could be attributed to a higher value of the clamped intensity, as the order of multiphoton absorption gradually increases from 3 at 1.3 μm to 5 at 2.4 μm [26].

Finally, in order to obtain an experimental nonlinear refractive index value, we have measured the energy transmission through 6H-SiC sample of 5 mm thickness. The transmission is affected by the nonlinear losses (multiphoton absorption and absorption by the free electron plasma), which increase significantly as the intensity of pump beam increases due to self-focusing, and which are the largest at the nonlinear focus. Therefore, the peak of the fractional losses (-dT/dE) derived from the transmission curve may be used to accurately determine the onset of filamentation, see [10] for details. The normalized energy transmission curve measured using pump pulses

OSA CONTINUUM

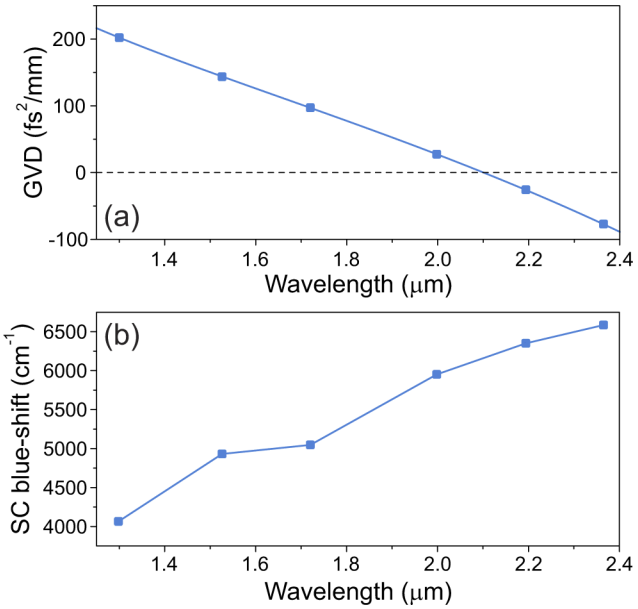

Fig. 4. (a) GVD of 6H-SiC and (b) spectral blue-shift of the SC versus the pump wavelength.

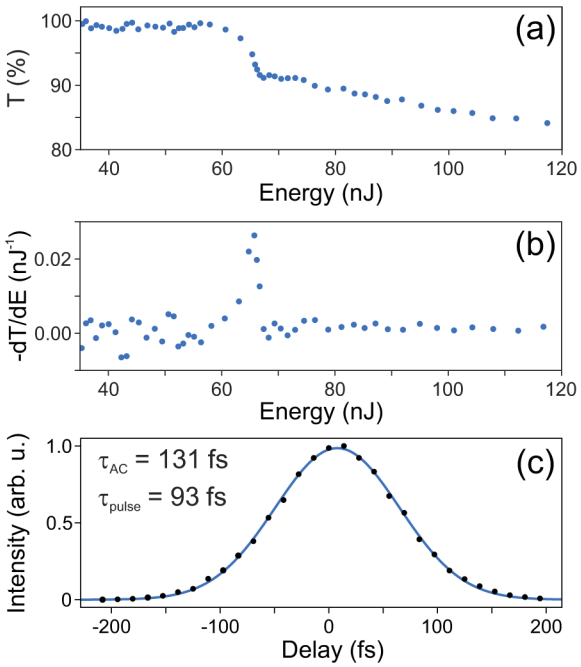

Fig. 5. (a) Normalized energy transmission of a 5 mm-thick 6H-SiC sample versus the pump pulse energy. (b) Fractional losses, where the maximum indicates that the nonlinear focus is positioned exactly at the output face of the sample. (c) Measured intensity autocorrelation function of 2.0 μm pump pulses.

OSA CONTINUUM

at 2.0 μm, is depicted in Fig. 5(a). Figure 5(b), shows the calculated fractional losses, with a peak at 66 nJ, indicating that the nonlinear focus is produced exactly at the output face of the sample. In other words, this suggests that the self-focusing distance is equal to the length of the sample (5 mm). Assuming the input parameters: the pulse duration of 93 fs at full width at half maximum, see Fig. 5(c), and the beam radius of 53 μm at the $1/e^2$ intensity level at the entrance face of the sample, measured by means of a knife method, and using the Marburger's law [39], we found a nonlinear refractive index value of $n_2 = 97 \pm 19 \times 10^{-16}$ cm^2/W, at 2.0 μm. The measured n_2 value agrees well with the expected one provided in Table 1 and the small discrepancy between the measured and calculated values could be attributed to the margin of error.

4. Conclusion

In conclusion, we have shown that 6H-SiC crystal is an excellent nonlinear material for supercontinuum generation in the near- to mid-infrared spectral region. We demonstrated the generation of smooth, more than an octave-spanning SC spectra produced by femtosecond filamentation in the normal, zero and anomalous GVD regions of the material. We also experimentally evaluated the nonlinear index of refraction of 6H-SiC at 2.0 μm by the measurement of nonlinear transmission and applying the Marburger's law. The obtained value ($n_2 = 97 \pm 19 \times 10^{-16}$ cm^2/W) coincides fairly well with the theoretically calculated one and is supported by the observed low energy thresholds for supercontinuum generation.

Funding. European Regional Development Fund (1.2.2-LMT-K-718-02-0017).

Acknowledgments. The authors thank Dr. Irmantas Kašalynas from Center for Physical Sciences and Technology for providing the 6H-SiC sample. This work has received funding from European Regional Development Fund (project No1.2.2-LMT-K-718-02-0017) under grant agreement with the Research Council of Lithuania (LMTLT).

Disclosures. The authors declare no conflicts of interest.

References

1. U. Megerle, I. Pugliesi, C. Schriever, C. F. Sailer, and E. Riedle, "Sub-50 fs broadband absorption spectroscopy with tunable excitation: putting the analysis of ultrafast molecular dynamics on solid ground," Appl. Phys. B **96**(2-3), 215–231 (2009).
2. G. Auböck, C. Consani, R. Monni, A. Cannizzo, F. Van Mourik, and M. Chergui, "Femtosecond pump/supercontinuum-probe setup with 20 kHz repetition rate," Rev. Sci. Instrum. **83**(9), 093105 (2012).
3. C. Calabrese, A. M. Stingel, L. Shen, and P. B. Petersen, "Ultrafast continuum mid-infrared spectroscopy: probing the entire vibrational spectrum in a single laser shot with femtosecond time resolution," Opt. Lett. **37**(12), 2265–2267 (2012).
4. P. Rigaud, A. Van de Walle, M. Hanna, N. Forget, F. Guichard, Y. Zaouter, K. Guesmi, F. Druon, and P. Georges, "Supercontinuum-seeded few-cycle mid-infrared OPCPA system," Opt. Express **24**(23), 26494–26502 (2016).
5. P. He, Y. Liu, K. Zhao, H. Teng, X. He, P. Huang, H. Huang, S. Zhong, Y. Jiang, S. Fang, X. Hou, and Z. Wei, "High-efficiency supercontinuum generation in solid thin plates at 0.1 TW level," Opt. Lett. **42**(3), 474–477 (2017).
6. A. Dubietis, G. Tamošauskas, R. Šuminas, V. Jukna, and A. Couairon, "Ultrafast supercontinuum generation in bulk condensed media," Lith. J. Phys. **57**(3), 113–157 (2017).
7. A. Dubietis and A. Couairon, *Ultrafast supercontinuum generation in transparent solid-state media* (Springer, 2019).
8. J. Darginavičius, D. Majus, V. Jukna, N. Garejev, G. Valiulis, A. Couairon, and A. Dubietis, "Ultrabroadband supercontinuum and third-harmonic generation in bulk solids with two optical-cycle carrier-envelope phase-stable pulses at 2 μm," Opt. Express **21**(21), 25210–25220 (2013).
9. M. Bradler, P. Baum, and E. Riedle, "Femtosecond continuum generation in bulk laser host materials with sub-μJ pump pulses," Appl. Phys. B **97**(3), 561–574 (2009).
10. A. Marcinkevičiūtė, G. Tamošauskas, and A. Dubietis, "Supercontinuum generation in mixed thallous halides KRS-5 and KRS-6," Opt. Mater. **78**, 339–344 (2018).
11. K. Liu, H. Liang, S. Qu, W. Li, X. Zou, Y. Zhang, and Q. J. Wang, "High-energy mid-infrared intrapulse difference-frequency generation with 5.3% conversion efficiency driven at 3 μm," Opt. Express **27**(26), 37706–37713 (2019).
12. S. Qu, G. C. Nagar, W. Li, K. Liu, X. Zou, S. H. Luen, D. Dempsey, K.-H. Hong, Q. J. Wang, Y. Zhang, B. Shim, and H. Liang, "Long-wavelength-infrared laser filamentation in solids in the near-single-cycle regime," Opt. Lett. **45**(8), 2175–2178 (2020).

OSA CONTINUUM

13. R. Šuminas, N. Garejev, A. Šuminienė, V. Jukna, G. Tamošauskas, and A. Dubietis, "Femtosecond filamentation, supercontinuum generation, and determination of n_2 in polycrystalline SBN," J. Opt. Soc. Am. B **37**(5), 1530–1534 (2020).
14. H. Liang, P. Krogen, R. Grynko, O. Novak, C.-L. Chang, G. J. Stein, D. Weerawarne, B. Shim, F. X. Kärtner, and K.-H. Hong, "Three-octave-spanning supercontinuum generation and sub-two-cycle self-compression of mid-infrared filaments in dielectrics," Opt. Lett. **40**(6), 1069–1072 (2015).
15. R. Šuminas, G. Tamošauskas, G. Valiulis, V. Jukna, A. Couairon, and A. Dubietis, "Multi-octave spanning nonlinear interactions induced by femtosecond filamentation in polycrystalline ZnSe," Appl. Phys. Lett. **110**(24), 241106 (2017).
16. R. Šuminas, A. Marcinkevičiūtė, G. Tamošauskas, and A. Dubietis, "Even and odd harmonics- semiconductors," J. Opt. Soc. Am. B **36**(2), A22–A27 (2019).
17. O. Mouawad, P. Béjot, F. Billard, P. Mathey, B. Kibler, F. Désévédavy, G. Gadret, J.-C. Jules, O. Faucher, and F. Smektala, "Filament-induced visible-to-mid-IR supercontinuum in a ZnSe crystal: Towards multi-octave supercontinuum absorption spectroscopy," Opt. Mater. **60**, 355–358 (2016).
18. K. Werner, M. G. Hastings, A. Schweinsberg, B. L. Wilmer, D. Austin, C. M. Wolfe, M. Kolesik, T. R. Ensley, L. Vanderhoef, A. Valenzuela, and E. Chowdhury, "Ultrafast mid-infrared high harmonic and supercontinuum generation with n_2 characterization in zinc selenide," Opt. Express **27**(3), 2867–2885 (2019).
19. A. Marcinkevičiūtė, V. Jukna, R. Šuminas, N. Garejev, G. Tamošauskas, and A. Dubietis, "Femtosecond filamentation and supercontinuum generation in bulk silicon," Opt. Lett. **44**(6), 1343–1346 (2019).
20. H. Sato, M. Abe, I. Shoji, J. Suda, and T. Kondo, "Accurate measurements of second-order nonlinear optical coefficients of 6H and 4H silicon carbide," J. Opt. Soc. Am. B **26**(10), 1892–1896 (2009).
21. F. De Leonardis, R. A. Soref, and V. M. Passaro, "Dispersion of nonresonant third-order nonlinearities in Silicon Carbide," Sci. Rep. **7**(1), 40924 (2017).
22. J. Cardenas, M. Yu, Y. Okawachi, C. B. Poitras, R. K. Lau, A. Dutt, A. L. Gaeta, and M. Lipson, "Optical nonlinearities in high-confinement silicon carbide waveguides," Opt. Lett. **40**(17), 4138–4141 (2015).
23. M. A. Guidry, K. Y. Yang, D. M. Lukin, A. Markosyan, J. Yang, M. M. Fejer, and J. Vučković, "Optical parametric oscillation in silicon carbide nanophotonics," Optica **7**(9), 1139–1142 (2020).
24. S. Wang, M. Zhan, G. Wang, H. Xuan, W. Zhang, C. Liu, C. Xu, Y. Liu, Z. Wei, and X. Chen, "4H-SiC: a new nonlinear material for midinfrared lasers," Laser Photonics Rev. **7**(5), 831–838 (2013).
25. H.-T. Fan, C.-H. Xu, Z.-H. Wang, G. Wang, C.-J. Liu, J.-K. Liang, X.-L. Chen, and Z.-Y. Wei, "Generation of broadband 17-μJ mid-infrared femtosecond pulses at 3.75 μm by silicon carbide crystal," Opt. Lett. **39**(21), 6249–6252 (2014).
26. A. Brodeur and S. Chin, "Band-gap dependence of the ultrafast white-light continuum," Phys. Rev. Lett. **80**(20), 4406–4409 (1998).
27. M. Durand, A. Jarnac, A. Houard, Y. Liu, S. Grabielle, N. Forget, A. Durécu, A. Couairon, and A. Mysyrowicz, "Self-guided propagation of ultrashort laser pulses in the anomalous dispersion region of transparent solids: a new regime of filamentation," Phys. Rev. Lett. **110**(11), 115003 (2013).
28. F. Silva, D. Austin, A. Thai, M. Baudisch, M. Hemmer, D. Faccio, A. Couairon, and J. Biegert, "Multi-octave supercontinuum generation from mid-infrared filamentation in a bulk crystal," Nat. Commun. **3**(1), 807 (2012).
29. S. Chekalin, A. Dormidonov, V. Kompanets, E. Zaloznaya, and V. Kandidov, "Light bullet supercontinuum," J. Opt. Soc. Am. B **36**(2), A43–A53 (2019).
30. M. J. Weber, *Handbook of optical materials*, vol. 19 (CRC press, 2002).
31. M. Sheik-Bahae, D. C. Hutchings, D. J. Hagan, and E. W. Van Stryland, "Dispersion of bound electron nonlinear refraction in solids," IEEE J. Quantum Electron. **27**(6), 1296–1309 (1991).
32. G. L. DesAutels, C. Brewer, M. Walker, S. Juhl, M. Finet, S. Ristich, M. Whitaker, and P. Powers, "Femtosecond laser damage threshold and nonlinear characterization in bulk transparent SiC materials," J. Opt. Soc. Am. B **25**(1), 60–66 (2008).
33. J. Leuthold, C. Koos, and W. Freude, "Nonlinear silicon photonics," Nat. Photonics **4**(8), 535–544 (2010).
34. X. Gai, Y. Yu, B. Kuyken, P. Ma, S. J. Madden, J. Van Campenhout, P. Verheyen, G. Roelkens, R. Baets, and B. Luther-Davies, "Nonlinear absorption and refraction in crystalline silicon in the mid-infrared," Laser Photonics Rev. **7**(6), 1054–1064 (2013).
35. T. Amotchkina, M. Trubetskov, D. Hahner, and V. Pervak, "Characterization of e-beam evaporated Ge, YbF_3, ZnS, and LaF_3 thin films for laser-oriented coatings," Appl. Opt. **59**(5), A40–A47 (2020).
36. D. E. Zelmon, D. L. Small, and R. Page, "Refractive-index measurements of undoped yttrium aluminum garnet from 0.4 to 5.0 μm," Appl. Opt. **37**(21), 4933–4935 (1998).
37. R. Adair, L. Chase, and S. A. Payne, "Nonlinear refractive index of optical crystals," Phys. Rev. B **39**(5), 3337–3350 (1989).
38. S. Xu, J. Qiu, T. Jia, C. Li, H. Sun, and Z. Xu, "Femtosecond laser ablation of crystals SiO_2 and YAG," Opt. Commun. **274**(1), 163–166 (2007).
39. J. H. Marburger, "Self-focusing: theory," Prog. Quantum Electron. **4**, 35–110 (1975).